Tanzania Journal of Science 50(5): 1077-1098, 2024
ISSN 0856-1761, e-ISSN 2507-7961

Mathematical Analysis of Monkeypox Transmission Dynamics with Control Strategies

Singo Juma Singo[1*,2], Furaha Michael Chuma[2], and Zubeda Seif Mussa[2]
[1]*Secondary Education Department, Geita Town Council, P. O. Box 384 Geita, Tanzania.*
[2]*Department of Physics, Mathematics, and Informatics, Dar es Salaam University College of Education, P. O. Box 2329 Dar es Salaam, Tanzania.*
[*] *Corresponding author, e-mail: singo.juma@yahoo.com*
Co-authors' e-mails: furaha.chuma@udsm.ac.tz, mussa.zubeda@udsm.ac.tz
Received 15 Aug 2024, Revised 4 Dec 2024, Accepted 17 Dec 2024, Published 30 Dec 2024
https://dx.doi.org/10.4314/tjs.v50i5.14

Abstract

This study develops a mathematical model to analyze the transmission dynamics of Monkeypox and evaluate the effectiveness of control strategies. The model is formulated as a system of nonlinear differential equations, capturing key factors such as human-to-human transmission, zoonotic reservoirs, and control measures like vaccination, culling, personal hygiene and treatment. The model's equilibrium points, including the disease-free and endemic equilibria, are determined and analyzed for stability using the effective reproduction number, R_e. Conditions under which $R_e < 1$ ensure the elimination of Monkeypox, while $R_e > 1$ indicates sustained transmission. A sensitivity analysis is performed to identify parameters that significantly influence R_e, such as the contact rate, effectiveness of control measures, and the rate of recovery. Numerical simulations demonstrate the impacts of individual control strategies such as vaccination, treatment, culling, and personal hygiene when applied alone. All of the control shows positive impact on the disease prevalence. This analysis provides critical insights for optimizing resource allocation and improving public health responses to Monkeypox outbreaks. The findings underscore the importance of timely and effective implementation of control measures to curb the spread of Monkeypox and mitigate its public health impact.

Keywords: Monkeypox; Personal Hygiene; Sensitivity Analysis; Vaccination; Treatment.

Introduction

Monkeypox (Mpox) is a zoonotic disease caused by a virus belonging to the *Poxviridae* family, *Chordopoxvirinae* subfamily, and genus *Orthopoxvirus* (Rahman et al. 2020, Peter et al. 2021, Heskin et al. 2022, Rizk et al. 2022). The disease is endemic in certain areas of West and Central Africa, particularly near forests where contact with wild animals is more likely (Usman and Adamu 2017, Peter et al. 2021, Rizk et al. 2022, Railian et al. 2023). Countries affected include the Democratic Republic of Congo, Cameroon, Liberia, the Central African Republic, Nigeria, Côte d'Ivoire, Gabon, and Sierra Leone (Peter et al. 2021, Velavan and Meyer 2022).

On May 21, 2022, the World Health Organization (WHO) reported 120 Mpox cases, of which 92 were confirmed and 28 were under investigation, from 12 countries, primarily in Europe and America. Additionally, 1,315 cumulative Mpox cases were reported from December 15, 2021, to May 1, 2022, across four African countries (Velavan and Meyer 2022, WHO 2022). The WHO also reported 57 deaths in the Democratic Republic of Congo and less than 5 deaths in Cameroon and Central African Republic (Velavan and Mayer 2022, WHO 2023).

There are two species of the Mpox virus, classified based on their geographical origins,

the West African and Central African species. These species cause human fatalities ranging from 3.6% to 10.6% (Martinez et al. 2022, Titanji et al. 2022, Velavan and Meyer 2022). Mpox primarily affects children and youths, with more severe cases observed in individuals with weakened immune systems (Rimoin et al. 2010, Hraib et al. 2022, Martinez et al. 2022, Seang et al. 2022, Titanji et al. 2022). The Mpox virus was first discovered in 1958 by Danish virologist Preben Alexander von Magnus in Copenhagen (Vera et al. 2022, Golden 2023).

The Mpox virus can be transmitted through human-to-human and animal-to-human transmissions (CDC 2022, Murphy and Ly 2022). Animal-to-human transmission occurs when infected animals such as primates, rodents, or pets bite humans or when humans come into direct contact with the fluids, blood, or raw meat of infected animals (Titanji et al. 2022, Beeson et al. 2023). Human-to-human transmission happens through sexual contact, direct contact with respiratory fluids, mucous membranes, skin lesions, or contaminated clothing or bedding of infected individuals (Usman and Adamu 2017, Titanji et al. 2022, Beeson et al. 2023, Diseases TLI 2023). Mpox typically takes one to two weeks from the initial day of infection for clinical signs to appear, however, in some cases, it may take up to three weeks (Usman and Adamu 2017, CDC-AFRICA 2022, Hraib et al. 2022, Luo and Han 2022, Shaheen et al. 2022). Early signs of Mpox include fever, headache, restlessness, and lymphadenopathy, while late signs include rashes of varying sizes, skin lesions, and swollen lymph nodes (Goyal 2022, Hraib et al. 2022).

Mathematical modeling plays a crucial role in analyzing the transmission dynamics of infectious diseases such as Mpox (Kermack and McKendrick 1927, Grassly and Fraser 2008, Brauer 2009, Badshah et al. 2013). Consequently, numerous studies have concentrated on developing mathematical models to understand Mpox transmission and evaluate control strategies. Such studies include Usman and Adamu (2017), who formulated and analyzed a transmission dynamics model for Mpox by incorporating treatment and vaccination control measures, and Somma et al. (2019), who developed and analyzed a mathematical model of Mpox transmission dynamics that included quarantine and public enlightenment campaigns as control strategies. Furthermore, Peter et al. (2021) examined the transmission dynamics of Mpox by incorporating the isolation of infected individuals as a control measure.

To the best of our knowledge, no study has incorporated personal hygiene as a control measure against the transmission dynamics of Mpox in human populations. Therefore, this study develops and analyzes a mathematical model for Mpox transmission dynamics, incorporating personal hygiene, treatment, vaccination, and culling of rodents to investigate their effectiveness in controlling the spread of Mpox.

Mathematical Model Development

A nonlinear deterministic mathematical model for the transmission dynamics of Mpox in human and rodent populations is developed. The model incorporates four control strategies: personal hygiene, treatment of humans, vaccination of humans, and culling of rodents. The human population N_h is divided into six compartments. Namely, Hygienic humans (H_h), Susceptible humans (S_h), Exposed humans (E_h), Infected humans (I_h), Recovered humans (R_h), and Vaccinated humans (V_h). Therefore, at any time, $N_h(t)=H_h(t)+S_h(t)+V_h(t)+E_h(t)+I_h(t)+R_h(t)$. On the other hand, the rodent population (N_r) is divided into Susceptible rodents (S_r) and Infected rodents (I_r) Hence, the total rodent population at any time is given by $N_r(t)=S_r(t)+I_r(t)$.

The model is developed based on the following assumptions:

(i) Individuals in the populations interact with each other freely and uniformly, with no significant barriers or separations between them.

(ii) After humans become infected with the disease and recover, they gain temporary immunity, but this immunity does not last indefinitely. As a result, these individuals eventually lose their

immunity and are considered susceptible to re-infection, and thus move back into the susceptible compartment of the model.

Humans are recruited at a rate Λ. Recruited humans are protected by adhering to personal hygiene rules and then enter the hygienic compartment at a proportion ε. The unprotected humans move to the susceptible compartment at a proportion of (1−ε). The hygienic humans who ignore hygiene protection are moved to the susceptible compartment at a rate ρ. The susceptible humans either get infected through human-to-human or rodent-to-human contact at a force of infection.

$$\lambda_h = \left(\frac{\beta I_h + \sigma I_r}{N_h}\right) \qquad (1)$$

Humans can either get vaccinated against the Mpox virus at a rate ν, or they may lose immunity after vaccination and return to the susceptible compartment at a rate τ. The infected humans remain in the exposed compartment for one to two weeks, during which they neither show clinical signs nor become infectious (Hraib et al. 2022, Luo and Han 2022, Shaheen et al. 2022). After two weeks, the exposed humans move to the infected compartment at a progression rate γ, becoming infectious and showing clinical signs of the Mpox virus. The infected humans in this compartment either die due to the disease at a rate ω or recover through treatment at a rate φ. The recovered humans, who lose immunity, return to the susceptible population at a rate δ. In each compartment, humans undergo natural death at a rate μ. Moreover, susceptible rodents are recruited at a rate Π and get infected through contact with infected rodents at a force of infection.

$$\lambda_r = \frac{\psi I_r}{N_r} \qquad (2)$$

Rodents are reduced due to natural death at a rate Φ and culling at a rate η. Furthermore, the infected rodents undergo disease-induced death rate α.

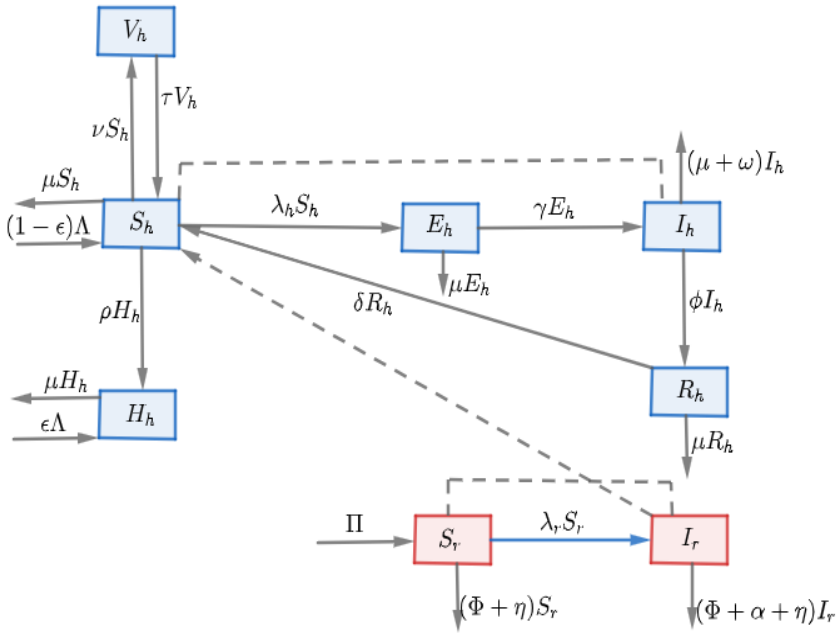

Figure 1: Schematic Representation of the Monkeypox Transmission Dynamics.

The model's non-linear differential equations are given as

$$
\begin{aligned}
\frac{dH_h}{dt} &= \varepsilon\Lambda - (\mu+\rho)H_h \\
\frac{dS_h}{dt} &= (1-\varepsilon)\Lambda + \rho H_h + \tau V_h + \delta R_h - (\lambda_h + \mu + \nu)S_h \\
\frac{dV_h}{dt} &= \nu S_h - (\tau+\mu)V_h \\
\frac{dE_h}{dt} &= \lambda_h S_h - (\mu+\gamma)E_h \\
\frac{dI_h}{dt} &= \gamma E_h + \tau V_h - (\mu+\omega+u_3)I_h \\
\frac{dR_h}{dt} &= \phi I_h - (\mu+\delta)R_h \\
\frac{dS_r}{dt} &= \Pi - (\lambda_r + \Phi + \eta)S_r \\
\frac{dI_r}{dt} &= \lambda_r S_r - (\Phi + \alpha + \eta)I_r
\end{aligned} \tag{3}
$$

With initial conditions: $H_h(0) > 0, S_h(0) > 0, V_h(0) > 0, E_h(0) \geq 0, I_h(0) \geq 0,$ $R_h(0) \geq 0, S_r(0) > 0, I_r(0) \geq 0.$

Basic Properties of the Model

Invariant regions and positivity of the solutions are the fundamental properties that make a mathematical model relevant for studying transmission dynamics of infectious diseases (Ayoade et al. 2019). Therefore, this section describes the satisfaction of the model system (3) with the aforementioned properties.

Positivity of the Solutions

The positivity of solutions is the model property that requires all solutions of the state variables to be positive $\forall t > 0$ given that the initial values are positive (Edward and Nyerere 2015, Mbuthia and Chepkwony 2019).

Theorem 1. The solutions of the state variables of model system (3) are such that $H_h(t) > 0,$ $S_h(t) > 0, V_h(t) > 0, E_h(t) > 0, I_h(t) > 0,$ $R_h(t) > 0,$ $S_r(t) > 0, I_r(t) > 0 \forall t > 0$ given that the initial values are positive.

Proof. Consider the first equation of the model system (3) given by

$$\frac{dH_h}{dt} = \varepsilon\Lambda - (\mu+\rho)H_h$$

It follows that

$$\frac{dH_h}{dt} \geq -(\mu+\rho)H_h \tag{4}$$

Separating variables in equation (4) gives

$$\frac{dH_h}{H_h} \geq -(\mu+\rho)dt \tag{5}$$

Integrating equation (5) on both sides gives

$$\int \frac{dH_h}{dt} \geq -\int (\mu+\rho)dt \tag{6}$$

Then

$$\ln H_h \geq -(\mu+\rho)t + C \tag{7}$$

where, C is the constant of integration When $t = 0, H_h = H_{0h}$, implies $C = \ln H_{0h}$, therefore

$$\ln H_h \geq -(\mu+\rho)t + \ln H_{0h} \tag{8}$$

Implies

$$H_h \geq H_{0h}\mathrm{e}^{-(\mu+\rho)t} > 0, \quad \forall t > 0 \text{ and } H_{0h} > 0.$$

By using a similar procedure, it is clear that $S_h > 0, V_h > 0, E_h > 0, I_h > 0, R_h > 0, S_r > 0,$ and $I_r > 0, \forall t > 0$. Therefore, solutions of state variables of the model system (3) are positive $\forall t > 0$, hence the model satisfies the positivity property of solutions.

Invariant Region of the Solutions

The invariant region of the solutions is the model property that requires the feasible region $\Theta = \{\mathbf{\Gamma}, \Omega\}$ of the model system (3) to make sense mathematically and biologically (Ayoade et al. 2019). Where Γ and Ω are feasible regions of the model in the human and rodent populations respectively. Since the developed model deals with human and rodent populations, all state variables and parameters are assumed to be positive $\forall t > 0$. Therefore, this subsection shows that the feasible region of the model system (3) remains positive $\forall t > 0$ and is globally attracted to the model.

Theorem 2. The feasible region $\mathbf{\Gamma} = \{(H_h, S_h, V_h, E_h, I_h, R_h) \in \mathbb{R}_+^6\}$ in the human population is positively invariant $\forall t > 0$ and globally attracted in $\mathbb{R}_+^6$.

Proof. From theorem 1, it is already shown that all solutions of the state variables in the human population are positive $\forall t > 0$. Then, it is supposed to show that the feasible region Γ is globally attracted in $\mathbb{R}_+^6$. Given that the total human population at any time is

$$N_h(t) = H_h(t) + S_h(t) + V_h(t) + E_h(t) + I_h(t) + R_h(t) \quad (9)$$

By differentiating equation (9) with respect to t, yields

$$\frac{dN_h}{dt} = \frac{dH_h}{dt} + \frac{dS_h}{dt} + \frac{dE_h}{dt} + \frac{dV_h}{dt} + \frac{dI_h}{dt} + \frac{dR_h}{dt} \quad (10)$$

Substitute the first to sixth equations of the model system (3) into equation (10) to get

$$\frac{dN_h}{dt} = \Lambda - \omega I_h - \mu\begin{pmatrix} H_h + S_h + E_h + V_h \\ +I_h + R_h \end{pmatrix} \quad (11)$$

But

$$H_h + S_h + E_h + V_h + I_h + R_h = N_h \quad (12)$$

Therefore

$$\frac{dN_h}{dt} = \Lambda - \omega I_h - \mu N_h \quad (13)$$

Then, equation (13) gives

$$\frac{dN_h}{dt} \leq \Lambda - \mu N_h \quad (14)$$

Implies

$$\frac{dN_h}{dt} + \mu N_h \leq \Lambda \quad (15)$$

Let $I.F = \mathrm{e}^{\int \mu dt}$ be the integrating factor of the equation (16), then $I.F = \mathrm{e}^{\mu t}$.

By multiplying $\mathrm{e}^{\mu t}$ on both sides of equation (15) gives

$$\mathrm{e}^{\mu t}\frac{dN_h}{dt} + \mathrm{e}^{\mu t}\mu N_h \leq \mathrm{e}^{\mu t}\Lambda \quad (16)$$

Then equation (16) gives

$$\frac{d(\mathrm{e}^{\mu t}N_h)}{dt} \leq \Lambda \mathrm{e}^{\mu t} \quad (17)$$

Implies

$$d(\mathrm{e}^{\mu t}N_h) \leq \Lambda \mathrm{e}^{\mu t} dt \quad (18)$$

Integrating equation (18) on both sides yields

$$\int d(\mathrm{e}^{\mu t}N_h) \leq \int \Lambda \mathrm{e}^{\mu t} dt \quad (19)$$

which results to

$$\mathrm{e}^{\mu t}N_h \leq \frac{\Lambda}{\mu}\mathrm{e}^{\mu t} + C \quad (20)$$

where C is the constant of integration. When $t = 0, N_h = N_{0h}$, implies $C = \frac{\mu}{\Lambda}N_{0h}$.

Now, substitute $C = \frac{\mu}{\Lambda}N_{0h}$ into equation (20) to get

$$e^{\mu t} N_h \leq \frac{\Lambda}{\mu} e^{\mu t} + \frac{\mu}{\Lambda} N_{0h} \quad (21)$$

Divide equation (21) throughout by $e^{\mu t}$ to get

$$N_h \leq \frac{\Lambda}{\mu} + \frac{\mu}{\Lambda} N_{0h} e^{-\mu t} \quad (22)$$

$$\text{As } t \to +\infty,\ N_h \leq \frac{\Lambda}{\mu} \quad (23)$$

Therefore, the feasible region $\Gamma = \{(H_h, S_h, E_h, V_h, I_h, R_h) \in \mathbb{R}_+^6 : 0 \leq N_h \leq \frac{\Lambda}{\mu}\}$ that is positively invariant $\forall t > 0$ and globally attracted in $\mathbb{R}_+^6$.

Theorem 3. The feasible region $\Omega = \{(S_r, I_r) \in \mathbb{R}_+^2\}$ in the rodent population is positively invariant $\forall t > 0$ and globally attracted in $\mathbb{R}_+^2$.

Proof. It also already shown that all state variables in the rodent population remain positive $\forall t > 0$, hence remains to show that Ω is globally attracted in $\mathbb{R}_+^2$. Given that the total rodent population at any time is given as

$$N_r(t) = S_r(t) + I_r(t) \quad (24)$$

By differentiating equation (24) with respect to t, gives

$$\frac{dN_r}{dt} = \frac{dS_r}{dt} + \frac{dI_r}{dt} \quad (25)$$

Substitute the seventh and eighth equations of the model system (3) into equation (25) leads to

$$\frac{dN_r}{dt} = \Pi - \alpha I_r - (\Phi + \eta)(S_r + I_r) \quad (26)$$

But $S_r + I_r = N_r$

Therefore

$$\frac{dN_r}{dt} = \Pi - \alpha I_r - (\Phi + \eta) N_r \quad (27)$$

Then, equation (27) becomes

$$\frac{dN_r}{dt} \leq \Pi - (\Phi + \eta) N_r \quad (28)$$

By rearranging equation (28) results

$$\frac{dN_r}{dt} + (\Phi + \eta) N_r \leq \Pi \quad (29)$$

Therefore

$$N_r \leq \frac{\Pi}{(\Phi+\eta)} + \frac{(\Phi+\eta)}{\Pi} N_{0r} e^{-(\Phi+\eta)t} \quad (30)$$

$$\text{As } t \to +\infty,\ N_r \leq \frac{\Pi}{(\Phi+\eta)} \quad (31)$$

Therefore, the feasible region $\Omega = \{(S_r, I_r) \in \mathbb{R}_+^2) : 0 \leq N_r \leq \frac{\Pi}{(\Phi+\eta)}\}$ in the rodent population is positively invariant $\forall t > 0$ and globally attracted in $\mathbb{R}_+^2$.

Conclusively, the feasible region $\Theta = \Gamma \times \Omega$ is positively invariant $\forall t > 0$ and globally attracted with respect to the model (3). Hence the model is mathematically meaningful and biologically well posed in Γ.

Existence of Equilibrium Points

An equilibrium point of a dynamical system is a solution that does not change with time (Arrowsmith et al. 1990). This means that the state variables of the dynamical system remain constant over time when the system is at equilibrium. The model system (3) has two equilibrium points: the disease-free and endemic equilibrium points. To get the equilibrium points, initially, the model system (3) is set to zero as follows

$$
\begin{aligned}
&\varepsilon\Lambda - (\mu+\rho)H_h = 0\\
&(1-\varepsilon)\Lambda + \rho H_h + \tau V_h + \delta R_h - (\lambda_h + \mu + \nu)S_h = 0\\
&\nu S_h - (\tau+\mu)V_h = 0\\
&\lambda_h S_h - (\mu+\gamma)E_h = 0\\
&\gamma E_h + \tau V_h - (\mu+\omega+u_3)I_h = 0\\
&\phi I_h - (\mu+\delta)R_h = 0\\
&\Pi - (\lambda_r + \Phi + \eta)S_r = 0\\
&\lambda_r S_r - (\Phi+\alpha+\eta)I_r = 0
\end{aligned}
\tag{32}
$$

Disease-Free Equilibrium Point

A disease-free equilibrium (DFE) point is an equilibrium point that is found when there is no infected individual in the population (Edward and Nyerere 2015, Upadhayay et al. 2022). Therefore, the DFE point of the model system (3) occurs when $I_h = E_h = I_r = R_h = 0$. Suppose $\varphi_0 = (H_h^0, S_h^0, V_h^0, E_h^0, I_h^0, R_h^0, S_r^0, I_r^0)$ is the DFE point of the model, then

$$
\begin{bmatrix} H_h^0 \\ S_h^0 \\ V_h^0 \\ E_h^0 \\ I_h^0 \\ R_h^0 \\ S_r^0 \\ I_r^0 \end{bmatrix} = \begin{bmatrix} \frac{\varepsilon\Lambda}{\mu+\rho} \\ \frac{(\tau+\mu)\Lambda(-\mu\varepsilon+\rho+\mu)}{\mu(\nu\rho+\nu\mu+\rho\tau+\rho\mu+\tau\mu+\mu^2)} \\ \frac{\nu\Lambda(-\mu\varepsilon+\rho+\mu)}{\mu(\nu\rho+\nu\mu+\rho\tau+\rho\mu+\tau\mu+\mu^2)} \\ 0 \\ 0 \\ 0 \\ \frac{\Pi}{\Phi+\eta} \\ 0 \end{bmatrix}
\tag{33}
$$

Also, at $\varphi_0, N_h^0 = H_h^0 + S_h^0 + V_h^0$, implies

$N_h^0 = \frac{\varepsilon\Lambda\mu(\nu\rho+\nu\mu+\rho\tau+\rho\mu+\tau\mu+\mu^2)+(\mu+\rho)\Lambda(-\mu\varepsilon+\rho+\mu)(\tau+\mu+\nu)}{\mu(\mu+\rho)(\nu\rho+\nu\mu+\rho\tau+\rho\mu+\tau\mu+\mu^2)}$,

and

$$N_r^0 = S_r^0 = \frac{\Pi}{\Phi+\eta}$$

Endemic Equilibrium Point

An endemic equilibrium (EE) point is an equilibrium point that is found when disease persists in the population (Neilan and Lenhart 2010, Ugwa et al. 2013, Peter et al. 2021). The values of the state variables of the model system at this point are nonzero (Ugwa et al. 2013). Therefore if $\varphi_1 = (H_h^*, S_h^*, V_h^*, E_h^*, I_h^*, R_h^*, S_r^*, I_r^*)$ is the EE point of the model system (3), then $(H_h^*, E_h^*, S_h^*, V_h^*, I_h^*, R_h^*, S_r^*, I_r^*) \neq (0,0,0,0,0,0,0,0)$. In this subsection, φ_1 is found by solving simultaneously the model equations in equation (33) (Ugwa et al. 2013). It follows that

$$H_h^* = \frac{\varepsilon\Lambda}{\mu+\rho},$$

$$S_h^* = \frac{\Lambda(1-\varepsilon)(\mu+\rho)(\mu+\delta)(\tau+\mu) + \rho\varepsilon\Lambda(\mu+\delta)(\tau+\mu) + \delta\varphi(\mu+\rho)(\tau+\mu)I_h^*}{((\lambda h+\mu+\nu)-\tau\nu)(\mu+\delta)(\mu+\rho)}$$

$$V_h^* = \frac{\nu\Lambda(1-\varepsilon)(\mu+\rho)(\mu+\delta)+\nu\rho\varepsilon\Lambda(\mu+\delta)+\nu\delta\varphi(\mu+\rho)I_h^*}{((\lambda h+\mu+\nu)-\tau\nu)(\mu+\delta)(\mu+\rho)}, \quad E_h^* = \frac{(\mu+\omega+\varphi)I_h^*}{\gamma},$$

$$I_h^* = \frac{\gamma\lambda h\Lambda(1-\varepsilon)(\mu+\rho)(\mu+\delta)(\tau+\mu)+\gamma\lambda h\rho\varepsilon\Lambda(\mu+\delta)(\tau+\mu)}{(\lambda h+\mu+\nu)-\tau\nu)(\mu+\delta)(\mu+\rho)(\mu+\gamma)(\mu+\omega+\varphi)-\gamma\lambda h\delta\varphi(\mu+\rho)(\tau+\mu)}, \quad R_h^* = \frac{\varphi I_h^*}{\mu+\delta},$$

$$S_r^* = \frac{\Pi}{\lambda_r + \Phi + \eta}, \quad \text{and} \quad I_r^* = \frac{\lambda_r \Pi}{(\lambda_r + \Phi + \eta)(\Phi + \alpha + \eta)}$$

where, $\lambda_h = \left(\frac{\beta I_h + \sigma I_r}{N_h}\right)$ *and* $\lambda_r = \frac{\psi I_r}{N_r}$

Effective Reproduction Number

The effective reproduction number R_e is the number of secondary infections produced when a single infected person is introduced into a whole susceptible population for an entire period of infection (Yan et al. 2014 Chitnis 2017, Perasso 2018, Fosu 2020, Olaniyi and Chuma 2023). The effective reproduction number is computed using the Next-Generation Matrix method (Yusuf and Benyah 2012, Mbuthia and Chepkwony 2019, Perasso 2018, Chuma and Mussa 2021, Majee et al. 2023). By this method, R_e is given as the maximum absolute value of the eigenvalues of the next-generation matrix (Chitnis 2017, Mbuthia and Chepkwony 2019, Onyejekwe et al. 2019, Chuma and Mussa 2021). To compute R_e of the model system (3), the model is grouped into new infections and rates of transfer.

For this case, the equations of the model system (3) with disease compartments are considered as given in equation (34)

$$\begin{aligned}
\frac{dE_h}{dt} &= \left(\frac{\beta I_h + \sigma I_r}{N_h}\right) S_h - (\mu + \gamma) E_h \\
\frac{dI_h}{dt} &= \gamma E_h + \tau V_h - (\mu + \omega + u_3) I_h \\
\frac{dI_r}{dt} &= \left(\frac{\psi I_r}{N_r}\right) S_r - (\Phi + \alpha + \eta) I_r \qquad (34)
\end{aligned}$$

Then, the system of equations in (34) is written in the form

$$\frac{dY}{dt} = \mathcal{F}(Y) - \mathcal{V}(Y)$$

where $Y = (E_h, I_h, I_r), \mathcal{F}(Y)$ is a function of new infections and $\mathcal{V}(Y)$ is a function of rates of transfer into and out of compartments.

Therefore,

$$\mathcal{F}(Y) = \begin{pmatrix} \left(\frac{\beta I_h + \sigma I_r}{N_h}\right) S_h \\ 0 \\ \left(\frac{\psi I_r}{N_r}\right) S_r \end{pmatrix}$$

$$\mathcal{V}(Y) = \begin{pmatrix} (\mu + \gamma) E_h \\ -\gamma E_h + (\mu + \omega + \phi) I_h \\ (\Phi + \alpha + \eta) I_r \end{pmatrix}$$

Then, matrices **F** and **V** are computed at the DFE point as follows

$\mathbf{F} = \left[\frac{\partial \mathcal{F}(Y)}{\partial (E_h, I_h, I_r)}\right]_{\varphi_0} = \begin{bmatrix} 0 & \frac{\beta S_h^0}{N_h^0} & \frac{\sigma S_h^0}{N_h^0} \\ 0 & 0 & 0 \\ 0 & 0 & \frac{\psi S_r^0}{N_r^0} \end{bmatrix}$ transfer out and into the system given that

$$S_h^0 = \frac{(\tau+\mu)\Lambda(-\mu\varepsilon+\rho+\mu)}{\mu(\nu\rho+\nu\mu+\rho\tau+\rho\mu+\tau\mu+\mu^2)},$$
$$N_h^0 = \frac{\varepsilon\Lambda\mu(\nu\rho+\nu\mu+\rho\tau+\rho\mu+\tau\mu+\mu^2)+(\mu+\rho)\Lambda(-\mu\varepsilon+\rho+\mu)(\tau+\mu+\nu)}{\mu(\mu+\rho)(\nu\rho+\nu\mu+\rho\tau+\rho\mu+\tau\mu+\mu^2)}$$

and

$$S_r^0 = N_r^0 = \frac{\Pi}{\Phi+\eta}$$

Therefore

$$\mathbf{F} = \begin{bmatrix} 0 & A_{12} & A_{13} \\ 0 & 0 & 0 \\ 0 & 0 & \psi \end{bmatrix}$$

Where

$$A_{12} = \frac{\beta\Lambda\lambda(\tau+\mu)(\mu+\rho)(-\mu\varepsilon+\rho+\mu)}{\varepsilon\lambda\mu\nu+\nu\mu+\rho\tau+\rho\mu+\tau\mu+\mu^2)+(\mu+\rho)\lambda(-\mu\varepsilon+\rho+\mu)(\tau+\mu+\nu)}$$
$$A_{13} = \frac{\sigma\Lambda\mu(\nu\nu+\nu\mu+\rho\tau+\rho\mu+\mu\mu+\mu+\mu)+(\mu\mu+\rho+\rho)\lambda(-\mu)+\rho+\mu)(\tau+\mu+\nu)}{\sigma\Lambda(\mu+\mu)(-\mu)}$$

Also

$$\mathbf{V} = \left[\frac{\partial\mathcal{V}(Y)}{\partial(E_h, I_h, I_r)}\right]_{\varphi_0} = \begin{bmatrix} \mu+\gamma & 0 & 0 \\ -\gamma & \mu+\omega+\phi & 0 \\ 0 & 0 & \Phi+\alpha+\eta \end{bmatrix}$$

Implies

$$\mathbf{V}^{-1} = \begin{bmatrix} \frac{1}{\mu+\gamma} & 0 & 0 \\ \frac{1}{(\mu+\gamma)(\mu+\omega+\phi)} & \frac{1}{\mu+\omega+\phi} & 0 \\ 0 & 0 & \frac{1}{\Phi+\alpha+\eta} \end{bmatrix}$$

The next-generation matrix $\mathbf{G} = \mathbf{F}\mathbf{V}^{-1}$ and is given as follows:

$$\mathbf{G} = \begin{bmatrix} A_{11} & A_{12} & A_{13} \\ 0 & 0 & 0 \\ 0 & 0 & \frac{\psi}{\Phi+\alpha+\eta} \end{bmatrix}$$

Where

$$A_{11} = \frac{\gamma\beta(\tau+\mu)((1-\varepsilon)\mu+\rho)}{(\tau+\nu+\mu)((\phi+\omega+\mu)(\gamma+\mu)\varepsilon\mu+(1-\varepsilon)\mu+\rho)}$$

$$A_{12} = \frac{\beta(\tau+\mu)((1-\varepsilon)\mu+\rho)}{(\tau+\nu+\mu)(\phi+\omega+\mu)\varepsilon\mu+((1-\varepsilon)\mu+\rho)}$$

$$A_{13} = \frac{\gamma\beta(\tau+\mu)((1-\varepsilon)\mu+\rho)}{(\tau+\nu+\mu)(\phi+\omega+\mu)\varepsilon\mu+((1-\varepsilon)\mu+\rho)}$$

Lastly, the eigenvalues of $\mathbf{G}$ can be found by taking $|\mathbf{G}-\lambda\mathbf{I}| = 0$ where $\mathbf{I}$ is 3×3 identity matrix. Hence

$$\begin{vmatrix} A_{11}-\lambda & A_{12} & A_{13} \\ 0 & 0-\lambda & 0 \\ 0 & 0 & \dfrac{\psi}{\Phi+\alpha+\eta}-\lambda \end{vmatrix} = 0$$

Gives:

$$\lambda_1 = \frac{\gamma\beta(\tau+\mu)((1-\varepsilon)\mu+\rho)}{(\tau+\nu+\mu)((\phi+\omega+\mu)(\gamma+\mu)\varepsilon\mu+(1-\varepsilon)\mu+\rho)},$$

$$\lambda_2 = 0, \text{ and}$$

$$\lambda_3 = \frac{\psi}{\Phi+\alpha+\eta}$$

Since R_e is the maximum absolute value of the eigenvalues of the next-generation matrix **G**, therefore $R_e = \max\{R_{eh}, R_{er}\}$ where R_{eh} and R_{er} are the effective reproduction numbers due to human and rodent populations respectively and they are given as:

$$R_{eh} = \frac{\gamma\beta(\tau+\mu)((1-\varepsilon)\mu+\rho)}{(\tau+\nu+\mu)((\phi+\omega+\mu)(\gamma+\mu)\varepsilon\mu+(1-\varepsilon)\mu+\rho)}$$

And

$$R_{0r} = \frac{\psi}{\Phi+\alpha+\eta}$$

Model Analysis

This section analyses the stability for both the disease-free equilibrium and the endemic equilibrium points. Sensitivity analysis is also carried out to determine the effects of change of the model parameters in R_e.

Stability of Disease-Free Equilibrium Point

The study uses the method by Castillo-Sharvez (2002), Castillo-Sharvez (2004), Chuma and Mwanga (2019), Peter et al. (2021), and Shao and Shateyi (2021) to analyse the global stability of the disease-free equilibrium point. By this method, the model equations are expressed in the form

$$\begin{aligned} \frac{dX}{dt} &= F(X,Y) \\ \frac{dY}{dt} &= G(X,Y) \end{aligned} \qquad (35)$$

Where $X \in \mathbb{R}^m$ whose elements are the number of uninfected individuals and $Y \in \mathbb{R}^n$ are the number of infected individuals for both infectious and incubation periods. The method states the necessary conditions that must be satisfied for the global asymptotic stability of the disease-free equilibrium. These conditions are stated as follows:

$S1$: $\frac{dX}{dt} = F(X,0)$, where X^0 is globally asymptotic stable.

$S2$: $G(X,Y) = BY - \hat{G}(X,Y)$, where $\hat{G}(X,Y) \geq 0$ for $(X,Y) \in \Theta$.

In this case, B is a matrix defined by $B = \left(\frac{\partial F(X^0,0)}{\partial Y}\right)$ whose off-diagonal elements must be non-negative and Θ is the invariant region of the model system (3).

Theorem 4. The disease-free equilibrium point is globally asymptotic stable if and only if $R_e < 1$ and conditions S1 and S2 are satisfied.

Proof. We are required to show that the model system (3) satisfies conditions $S1$ and $S2$ at the disease-free equilibrium point. From the model, $X = (H_h, S_h, V_h, R_h, S_r)$ and $Y = (E_h, I_h, I_r)$. Therefore

For condition 1 :

$$F(X,0)=\begin{pmatrix}\varepsilon\Lambda-(\mu+\rho)H_h\\(1-\varepsilon)\Lambda+\rho H_h+\delta R_h+\tau V_h-(\mu+\nu)S_h\\\nu S_h-(\tau+\mu)V_h\\-(\mu+\delta)R_h\\\Pi-(\Phi+\eta)S_r\end{pmatrix} \tag{36}$$

It follows that the Jacobian matrix of $F(X^0,0)$ is given by

$$J_{\varphi_0}=\begin{bmatrix}-(\mu+\rho)&0&0&0&0\\\rho&-(\mu+\nu)&\tau&\delta&0\\0&\nu&-(\tau+\mu)&0&0\\0&0&0&-(\mu+\delta)&0\\0&0&0&0&-(\Phi+\eta)\end{bmatrix} \tag{37}$$

The eigenvalues of the matrix in equation (37) are:

$\lambda_1=-(\mu+\rho),\lambda_2=-(\mu+\nu),\lambda_3=-\frac{\mu(\nu+\tau+\mu)}{\mu+\nu},\lambda_4=-(\mu+\delta),\lambda_5=-(\Phi+\eta).$

Since all eigenvalues are negative, then X^0 is globally asymptotic stable, hence the condition *SI* satisfies.

For condition $S2$

$$G(X,Y)=\begin{pmatrix}\frac{(\beta I_h+\sigma I_r)}{N_h}S_h-(\mu+\gamma)E_h\\\gamma E_h-(\mu+\omega+\phi)I_h\\\frac{\psi I_r}{N_r}S_r-(\Phi+\alpha+\eta)I_r\end{pmatrix} \tag{38}$$

Then

$$B=\left[\frac{\partial G(X^0,0)}{\partial Y}\right]_{\varphi_0}=\begin{bmatrix}-(\mu+\gamma)&\frac{\beta S_h^0}{N_h}&\frac{\sigma S_h^0}{N_h}\\\gamma&-(\mu+\omega+\phi)&0\\0&0&\frac{\psi S_r^0}{N_r}-(\Phi+\alpha+\eta)\end{bmatrix} \tag{39}$$

From equation (39), it is clearly shown that all off-diagonal elements of matrix B are nonnegative.

Also

$$\hat{G}(X,Y)=\begin{pmatrix}(\beta I_h+\sigma I_r)\left(1-\frac{S_h}{N_h}\right)\\0\\\psi I_r\left(1-\frac{S_r}{N_r}\right)\end{pmatrix} \tag{40}$$

Implies, $\hat{G}(X,Y)\geq 0$ given that $0\leq S_h\leq N_h$ and $0\leq S_r\leq N_r$.

Since, all off-diagonal elements of the matrix B are non-negative and $\hat{G}(X,Y)\geq 0$, then the model satisfies condition $S2$.

Generally, the model system (3) satisfies both conditions $S1$ and $S2$ therefore by theorem 4, the disease-free equilibrium point φ_0 is globally asymptotic stable when $R_e<1$.

Stability of Endemic Equilibrium Point

The study analyses the stability of the endemic equilibrium point by using the Lyapunov theorem. The theorem provides the necessary and sufficient conditions for the global stability of the endemic equilibrium point (Syafruddin and Noorani 2013, Yan et al. 2014, Agarana and Bishop 2015, Barro et

al. 2018, Bezabih et al. 2020, Chuma and Mussa 2021, Liana and Chuma 2023). That is, the endemic equilibrium point is said to be globally asymptotic stable if there exists a function S called the Lyapunov function such that:

i) S is positive definite.
ii) $\dot{S}(X) < 0 \; \forall X \neq 0, \dot{S}(0) = 0.$

And, $X = (S_h, H_h, V_h, E_h, I_h, R_h, S_r, I_r)$.

Theorem 5. The endemic equilibrium point is said to be globally asymptotic stable if and only if $R_e > 1$.

Proof. Required to show that $\varphi_1 = (S_h^*, H_h^*, V_h^*, E_h^*, I_h^*, R_h^*, S_r^*, I_r^*)$ satisfy the Lyapunov necessary and sufficient conditions. Consider the Lyapunov function of the Goh Volterra type given by

$$S = \left(H_h - H_h^* - H_h^* \ln \frac{H_h}{H_h^*}\right) + \left(S_h - S_h^* - S_h^* \ln \frac{S_h}{S_h^*}\right) + \left(V_h - V_h^* - V_h^* \ln \frac{V_h}{V_h^*}\right)$$
$$+A\left(I_h - I_h^* - I_h^* \ln \frac{I_h}{I_h^*}\right) + \left(S_r - S_r^* - S_r^* \ln \frac{S_r}{S_r^*}\right) + \left(I_r - I_r^* - I_r^* \ln \frac{I_r}{I_r^*}\right) + \left(R_h - R_h^* - R_h^* \ln \frac{R_h}{R_h^*}\right) \quad (41)$$

From equation (41) S is positive definite hence Lyapunov's first condition satisfies.

Differentiating function (41) and substituting $\dot{H}_h, \dot{S}_h, \dot{E}_h, \dot{V}_h, \dot{I}_h, \dot{S}_r, \dot{I}_h$ and $\dot{R}_r$ from system (3) into function (41) at disease free equilibrium point, with simplifications, leads to:

$$\dot{S} \leq (\mu + \rho)H_h^* \left(2 - \frac{H_h}{H_h^*} - \frac{H_h^*}{H_h}\right) + (\Phi + \eta)S_r^* \left(2 - \frac{S_r}{S_r^*} - \frac{S_r^*}{S_r}\right) + \frac{\psi I_r^* S_r^*}{N_r}\left(2 - \frac{S_r^*}{S_r} - \frac{S_r}{S_r^*}\right) \quad (42)$$

From equation (42), $\dot{S}(X) < 0 \quad \forall X \neq 0$ and $\dot{S}(0) = 0$ if and only if $H_h = H_h^*, S_h = S_h^*, E_h = E_h^*, I_h = I_h^*, S_r = S_r^*, R_h = R_h^*$, and $V_h = V_h^*$. Also, as $\mathrm{t} \to \infty, H_h \to H_h^*, S_h \to S_h^*, E_h \to E_h^*, I_h \to I_h^*, S_r \to S_r^*, R_h \to R_h^*$ and $V_h \to V_h^*$. According to LaSalle (1976) and Olaniyi and Chuma (2023) $\dot{S} = 0$ is a singleton therefore an endemic equilibrium point φ_1 is globally asymptotic stable whenever $R_e > 1$.

Sensitivity Analysis of the Model

In epidemiological models, sensitivity analysis refers to the analysis of state variables about the change of model parameters (Gumel 2012, Olaniyi et al. 2016, Masoumnezhad et al. 2020, Somma and Akinwande 2020, Alshomrani et al. 2021, Rangasamy et al. 2022, Sudarmaji et al. 2022). Sensitivity analysis helps to determine the influence of each parameter in spreading infectious diseases. Since the effective reproduction number R_e provides the threshold condition for disease persistence, this section examines the effects of change of parameters in R_{eh}. This is done by using the normalized forward sensitivity index method which is defined as the partial derivative of R_{eh} with respect to the model parameter times the parameter divided by R_{eh} (Olaniyi et al. 2016, Somma and Akinwande 2020, Alshomrani et al. 2021, Alshomrani et al. 2023, McCollum et al 2023, Olaniyi and Chuma 2023). Suppose p is any parameter in R_{eh} and $\mathcal{N}$ is the sensitivity index of R_{eh} with respect to p, then

$$\mathcal{N}_p^{R_{eh}} = \left(\frac{\partial R_{eh}}{\partial p}\right)\frac{p}{R_{eh}} \quad (43)$$

Using the definition (43), the sensitivity indices of R_{eh} with respect to each parameter are as follows

$$
\begin{aligned}
\mathcal{N}_{\beta}^{R_{eh}} &= \frac{\partial R_{eh}}{\partial \beta} \times \frac{\beta}{R_{eh}} = 1 \\
\mathcal{N}_{\rho}^{R_{eh}} &= \frac{\partial R_{eh}}{\partial \rho} \times \frac{\rho}{R_{eh}} = 0.003257 \\
\mathcal{N}_{\mu}^{R_{eh}} &= \frac{\partial R_{eh}}{\partial \mu} \times \frac{\mu}{R_{eh}} = -0.778038 \\
\mathcal{N}_{\varepsilon}^{R_{eh}} &= -\frac{\partial R_{eh}}{\partial \varepsilon} \times \frac{\varepsilon}{R_{eh}} = -0.057535 \\
\mathcal{N}_{\omega}^{R_{eh}} &= \frac{\partial R_{eh}}{\partial \omega} \times \frac{\omega}{R_{eh}} = -0.010029 \\
\mathcal{N}_{\nu}^{R_{eh}} &= \frac{\partial R_{eh}}{\partial \nu} \times \frac{\nu}{R_{eh}} = -0.799041 \\
\mathcal{N}_{\phi}^{R_{0h}} &= \frac{\partial R_{eh}}{\partial \phi} \times \frac{\phi}{R_{eh}} = -0.026492 \\
\mathcal{N}_{\Lambda}^{R_{eh}} &= \frac{\partial R_{eh}}{\partial \Lambda} \times \frac{\Lambda}{R_{eh}} = 8.650414 \times 10^{-10}
\end{aligned}
\tag{44}
$$

Similarly, by applying the procedure in equation (43) the sensitivity index of R_{eh} with respect to γ can be computed. The results obtained in equation (44) show that some sensitivity indices have positive results while others have negative results. The positive sign of the result indicates that an increase or decrease of the parameter is directly proportional to the increase or decrease of R_{eh}. While the negative sign indicates that an increase or decrease of the parameter is inversely proportional to the increase or decrease of R_{eh}.

T

able 1: Description of Model Parameters

Parameter	Parameter Description	Values ($Year^{-1}$)	Source
Λ	Humans' recruitment rate	0.029	Leandry (2022)
μ	Humans' natural death rate	0.094	Assumed
Ω	Humans' disease-induced death rate	0.2	Peter et al. (2021)
B	Human-to-human transmission coefficient	0.00006	Peter et al. (2021)
Σ	Human-to-rodent transmission coefficient	0.00025	Peter et al. (2021)
Γ	Humans' progression rate	0.2	Peter et al. (2021)
E	Hygienic practices rate of humans	0.3	Assumed
N	Vaccination rate of susceptible humans	0.1	Leandry (2022)
Φ	Treatment rate of infected humans	0.83	Leandry (2022)
P	Loss of protection of hygienic humans	0.003	Assumed
Δ	Loss of immunity of recovered humans	0.00023	Assumed
T	Loss of immunity of vaccinated humans	0.003	Leandry (2022)
Π	Rodents' recruitment rate	0.2	Leandry (2022)
Ψ	Rodent-to-rodent transmission coefficient	0.027	Peter et al. (2021)
Φ	Rodents' natural death rate	0.002	Peter et al. (2021
A	Rodents' disease-induced death rate	0.5	Leandry (2022)

H	Culling rate of the rodents	0.3	Assumed

Numerical Results and Discussion

This section presents numerical simulations to investigate the transmission dynamics of the Mpox model and the effects of control strategies against the transmission dynamics of Mpox in the human population. This is performed by the use of parameter values given in Table 1 and the following initial values: $H_h(0) = 200, S_h(0) = 1000, V_h(0) = 300,\ E_h(0) = 150, I_h(0) = 50, R_h(0) = 80,\ S_r(0) = 200,$ and $I_r(0) = 50$. MATLAB R2013b with Ode45 solver codes was applied to perform the numerical and graphical solutions.

Numerical Simulations of the Basic Mpox Model

Figure 1 shows that the trajectories of hygienic, susceptible, exposed, and infected humans decrease exponentially from initial values and then converge to zero at different times. Likewise, the trajectories of the vaccinated and recovered humans start to increase and reach a certain maximum value before converging to zero. This implies that the transmission dynamics of Mpox in the human population can be eliminated by the application of personal hygiene, vaccination, treatment, and culling of rodents' control measures.

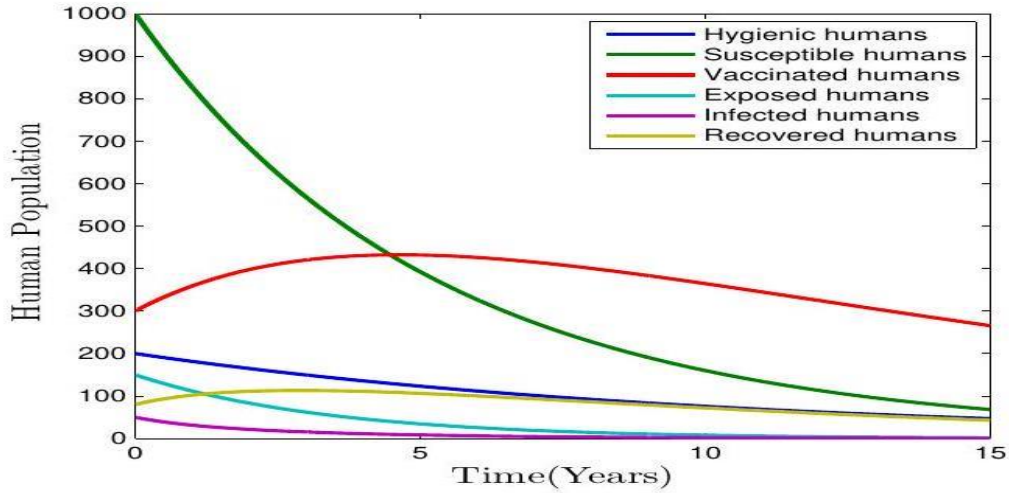

Figure 2: Transmission Dynamics of the Mpox in the Human Population.

Also, Figure 3 indicates the transmission dynamics of Mpox in the rodent population. The figure shows that the trajectories of susceptible and infected rodents converge at different times whereby the trajectory of the susceptible rodents converges faster than that of infected rodents. This also implies that the transmission dynamics of Mpox in the rodent population can be eliminated by the application of personal hygiene, vaccination, treatment, and culling of rodent control measures.

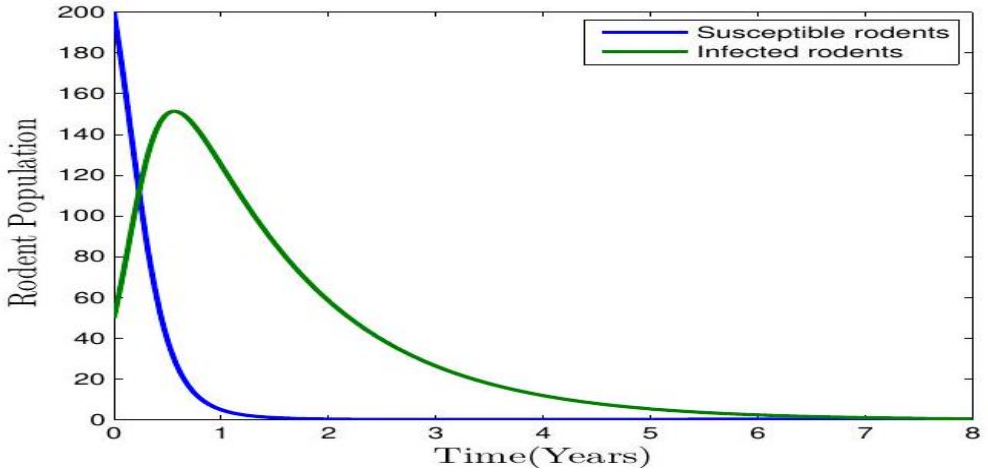

Figure 3: Transmission Dynamics of the Mpox in the Rodent Population.

According to, Figures 2 and 3 the number of infected humans and rodents converges faster after incorporating two control measures, such as practicing personal hygiene and culling rodents than just applying vaccination and treatment control measures, as in the work of Usman and Adamu (2017).

Numerical Simulation of R_{eh}

This section performs the numerical simulation of R_{eh} versus the model parameters β, ε and ν. These parameters and their respective sensitivity indices are: $\beta = 1, \varepsilon = -0.057535$ and $\nu = -0.79904$.

Figure 4 shows that the magnitude of R_{eh} increases as the parameter value of β increases. This implies that the parameter has more influence on increasing the value of R_{eh}. Therefore, the appropriate control measures should be applied to reduce its value.

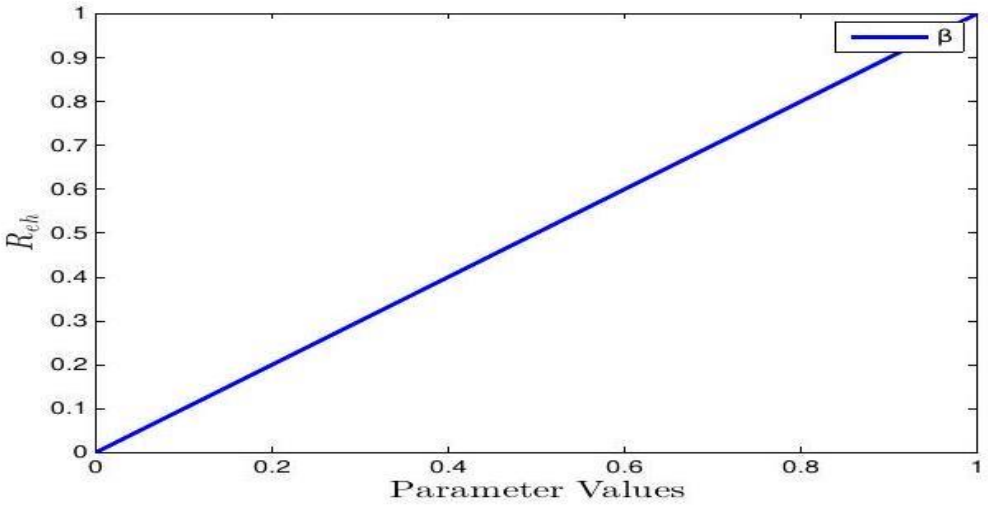

Figure 4: Trajectories of R_{eh} versus β.

On the other hand, Figure 5 shows that R_{eh} decreases as the parameter values of ε and ν increase. This implies that the parameters ε and ν have more influence on decreasing the value of R_{eh}. Therefore, the rate of practicing personal hygiene ε and vaccination of humans ν should be increased to lower the value of R_{eh}. This is contrary to the study of Usman

and Adamu (2017) who incorporated only vaccination as a preventive measure.

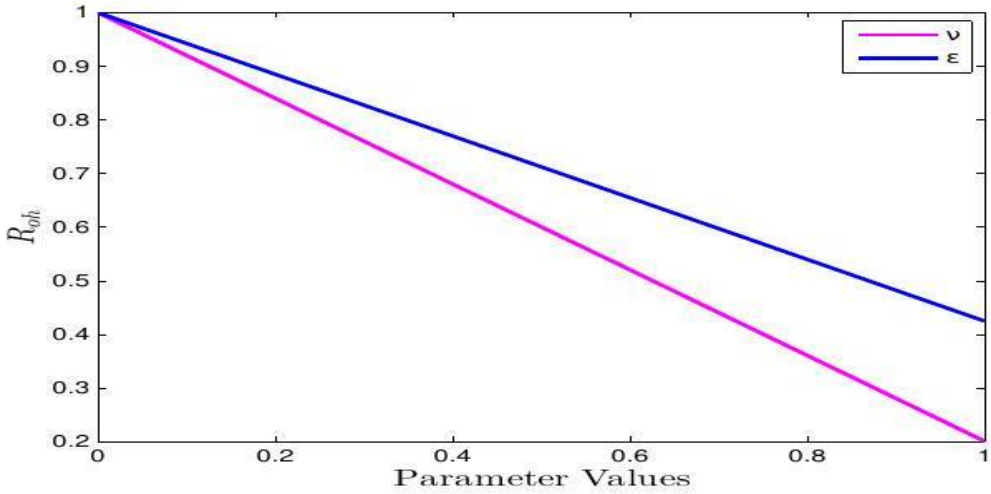

Figure 5: Trajectories of R_{eh} versus Model Parameters: ν and ε.

Effects of Control Strategies during the Outbreak

This section presents numerical simulations to show the effect of each control strategy by varying its parameter value during the Mpox outbreak. Other studies such as Usman and Adamu (2017), Somma et al. (2019), and Peter et al. (2021) did not perform the role of effect of each control measure by varying parameter values.

Effects of Vaccination on the Susceptible Humans

Figure 6 shows trajectories of susceptible humans by varying the rate of vaccination (ν). The figure shows that the trajectory converges fast when the rate of vaccination increases. This implies that to reduce the large number of humans who are at risk of being infected by the Mpox virus, the rate of vaccination should be increased.

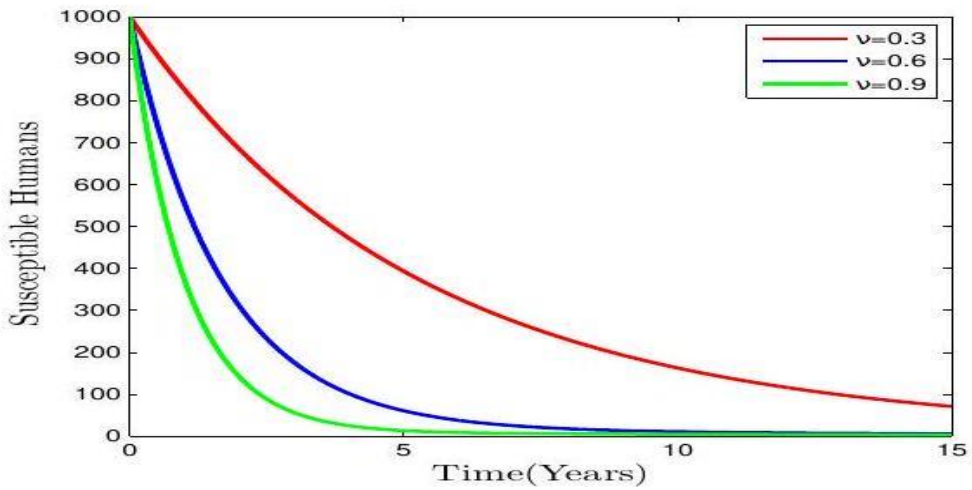

Figure 6: Effects of Vaccination on the Susceptible Humans.

Effects of Treatment on the Human Population.

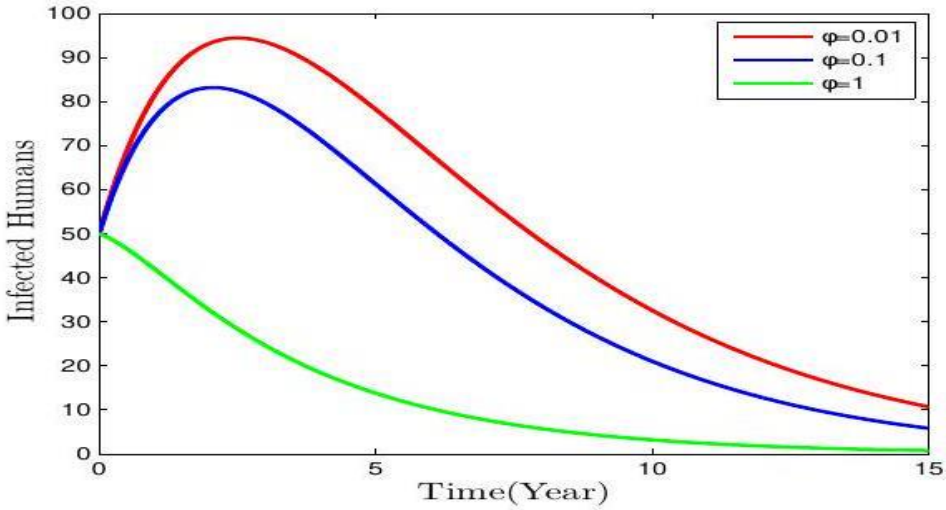

Figure 7: Effects of Treatment on the Infected Humans.

Figure 7 shows the trajectories of the infected humans as the treatment rate (φ) varies. The figure shows that the trajectory converges fast as the rate of treatment increases. This means that to control the population free from disease in a short period the rate of treatment of infected humans should be increased.

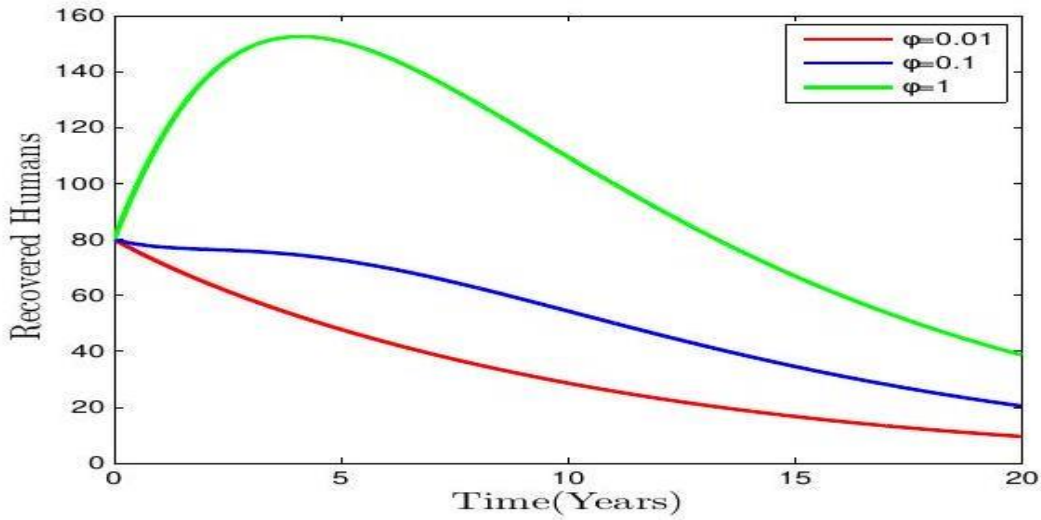

Figure 8: Effects of Treatment on the Recovered Humans.

Furthermore, Figure 8 shows the trajectories of the recovered humans by varying the rate of treatment (φ) of the infected humans. The figure shows that the trajectory of the number of recovered humans increases fast as the rate of treatment increases. This implies that to increase the large number of recovered humans in a short period the rate of treatment of infected humans should be increased.

Effects of Personal Hygiene on Susceptible Humans

Figure 9 shows the trajectories of the number of susceptible humans by varying rates of practicing personal hygiene (ε). The trajectory converges fast as the rates of personal hygiene increase. This implies that to protect the large number of humans from the Mpox virus the rate of practicing personal hygiene should be increased.

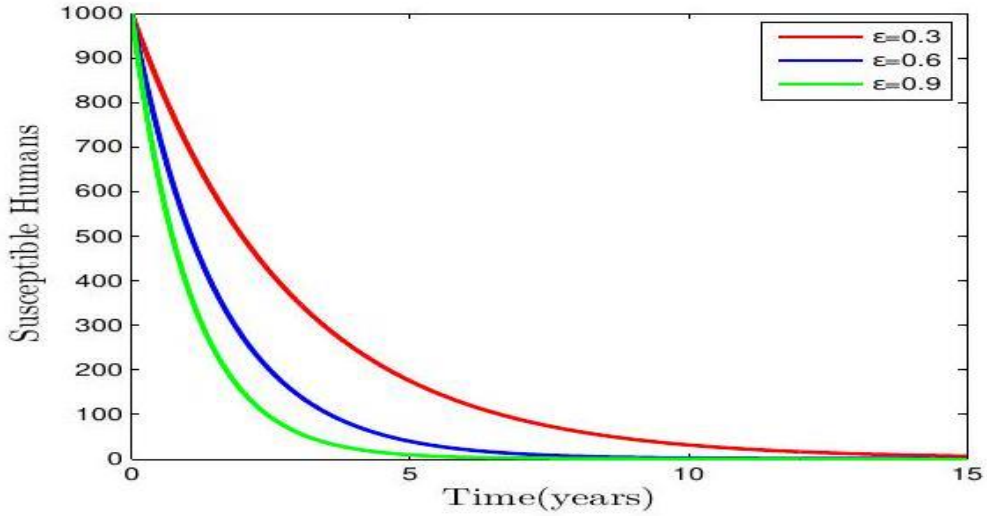

Figure 9: Effects of Personal Hygiene on the Susceptible Humans.

Effects of Culling on Infected Rodents

Figure 10 shows the trajectories of the infected rodents by varying rates of culling rodents. The figure shows that the trajectory converges fast as the rate of culling rodents (η) increases.

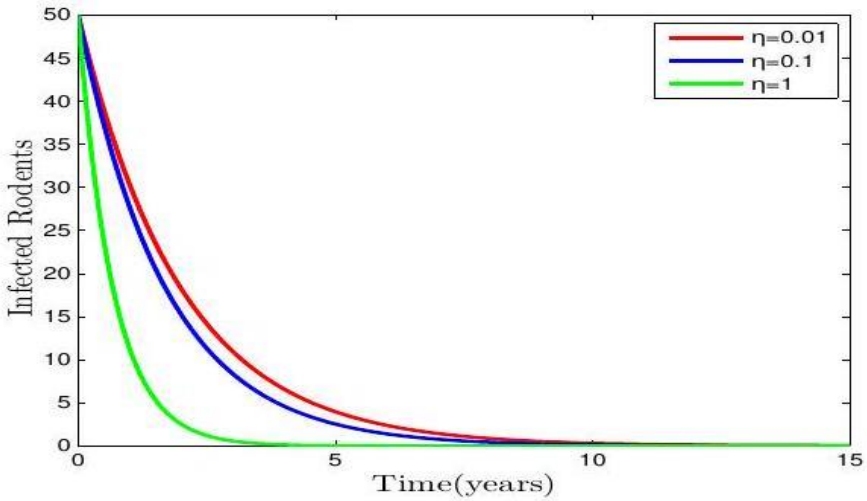

Figure 10: Effects of Culling on the Infected Rodents.

This implies that an increase in the rate of culling rodents reduces the number of infected rodents quickly, reducing the rodent-human contact rate.

Conclusion

The current study aimed to develop and analyze a mathematical model of the

transmission dynamics of Mpox with control strategies. This model was designed to represent the transmission dynamics of Mpox in human and rodent populations and incorporated four control strategies: personal hygiene, vaccination, treatment, and culling. The fundamental properties of the model were examined to ensure it is mathematically and biologically sound. The effective reproduction number was calculated using the Next-Generation Matrix method. Stability analysis of the disease-free equilibrium point was performed using the method by Castillo-Chávez (2002), while the stability of the endemic equilibrium point was analyzed using the Lyapunov function. The results indicated that, under the specified conditions, the disease-free equilibrium point is stable when $R_e < 1$ and unstable when $R_e < 1$.

Furthermore, the study performed numerical simulations to explore the basic Mpox model and the effects of control measures on the spread of Mpox in the human population. The results showed that each control measure: personal hygiene, vaccination of susceptible humans, treatment of infected individuals, and culling of rodents can eliminate the transmission dynamics of Mpox in humans. Moreover, this study recommends that future research delve deeper into the transmission dynamics of Mpox disease, particularly by investigating the effects of media and the cost-effectiveness of implemented control measures.

Acknowledgements

The authors acknowledge all reviewers for their good comments and suggestions that helped to improve this article.

References

Agarana MC and Bishop SA 2015 Quantitative analysis of equilibrium solution and stability for non-linear differential equation governing pendulum clock. *Int. J. Appl. Eng. Res.* 10(24):44112–44117.

Al-shomrani AS, Ullah MZ and Baleanu D 2021 Caputo SIR model for COVID-19 under optimized fractional order. *Adv. Different. Equat* 2021(1): 185

Al Shomrani MM, Musa SS and Yusuf A 2023.Unfolding the transmission dynamics of monkeypox virus: An epidemiological modelling analysis. *Mathematics*. 11(5): 1121.

Arrowsmith DK, Place CM, Place C, et al. 1990 An Introduction to Dynamical Systems, Cambridge University Press, Cambridge.

Ayoade A, Ibrahim M, Peter O and Amadiegwu S 2019 On validation of an epidemiological model. *J. Fundament. Appl. Sci*. 11(2): 578–586.

Badshah V, Porwal P and Tiwari V 2013 Mathematical modeling and role of dynamics in epidemiology. *Health*. 22: 23–24.

Barro M, Guiro A and Ouedraogo D 2018 Optimal control of a sir epidemic model with general incidence function and time delays. *Cubo (Temuco)*. 20 (2): 53–66.

Beeson A, Styczynski A, Hutson CL, Whitehill F, Angelo KM, Minhaj FS and others 2023 Mpox respiratory transmission: the state of the evidence. *Lancet Microbe*. 4: 277–283.

Bezabih AF, Edessa GK and Koya PR 2020 Mathematical eco-epidemiological model on prey-predator system. *Math. Model. Appl.* 5(3): 183–190.

Brauer F 2009 Mathematical epidemiology is not an oxymoron. *BMC Public Health*. 9(1): 1–11.

Castillo-Chavez C 2002 On the computation of r. and its role on global stability Carlos Castillo-Chavez*, Zhilan Feng, and Wenzhang Huang. *Math. Approach. Emerg Reemerg Infect. Dis: an Introduction*. 1: 229.

Castillo-Chavez C and Song B 2004 Dynamical models of tuberculosis and their applications. *Math. Biosci. Eng.*1(2): 361–404.

CDC 2022 Monkeypox treatment. Accessed at https://www.cdc.gov/poxvirus/monkeypox/ clinicians/treatment.htm/.

CDC-AFRICA 2022 Outbreak brief 4: Monkeypox in Africa Union Member States. Available at https://africacdc.org.

Chitnis N 2017 Introduction to SEIR models. In Workshop on Mathematical Models of Climate Variability, *Environmental*

Change and Infectious Diseases, Trieste, Iitaly.

Chuma FM and Mwanga GG 2019 Stability analysis of equilibrium points of Newcastle disease model of village chicken in the presence of wild birds reservoir. *Int. J. Math. Sci. Comput*. 5(2): 1–18.

Chuma F and Mussa Z 2021 Campylobacteriosis transmission dynamics in humans: Modeling the effects of public health education, treatment, and sanitation. *Tanzania J. Sci*. 47(1): 315–331.

Diseases TLI 2023 A tale of potential Mpox reinfection. *Lancet. Infect. Dis*. 23: 508–509.

Edward S and Nyerere N 2015 A mathematical model for the dynamics of cholera with control measures. *Applied and Computational Mathematics*.4(2):53–63.

Fosu GO, Akweittey E and Adu-Sackey A 2020 Next-generation matrices and basic reproductive numbers for all phases of the coronavirus disease. *Open J. Math. Sci*. 4(1): 261–272.

Golden J, Harryman L, Crofts M, Muir P, Donati M, Gillett S, and Irish C 2023 Case of apparent Mpox reinfection. *Sexually Transmitted Infections*. 99(4): 283–284.

Goyal L, Ajmera K, Pandit R and Pandit T 2022 Prevention and treatment of monkeypox: A step-by-step guide for healthcare professionals and the general population. *Cureus*. 14(8).

Grassly NC and Fraser C 2008 Mathematical models of infectious disease transmission. *Nat. Rev. Microbiol*. 6(6): 477–487.

Gumel AB 2012 Causes of backward bifurcations in some epidemiological models. *J. Math. Anal. Appl.* 395 (1):355–365.

Heskin J, Belfield A, Milne C, Brown N, Walters Y, Scott C, Bracchi M, Moore L, Mughal N, Rampling T, Winston A, Nelson M, Duncan S, Jones R, Price DA, and Mora-Peris B 2022 Transmission of monkeypox virus through sexual contact–a novel route of infection. *J. Infect.* 85(3): 334–363.

Hraib M, Jouni S, Albitar MM, Alaidi S and Alshehabi Z 2022 The outbreak of monkeypox 2022: An overview. *Ann. Med. Surgery*. 79: 104069-104073.

Kermack WO and McKendrick AG 1927 A contribution to the mathematical theory of epidemics. *Proc. Royal Soc. London. Series A, Containing Papers of a Mathematical and Physical Character*. 115(772): 700–721.

LaSalle JP1976 The stability of dynamical systems. *Zhonghuai Wu Yueyang Vocational Technical College Yueyang, Hunan*. 414000.

Leandry L 2022 An investigation on the monkeypox virus dynamics in human and rodent populations for a deterministic mathematical model. *Inform. Med. Unlock.* 41 (2023): 101325.

Liana YA and Chuma FM 2023 Mathematical modeling of giardiasis transmission dynamics with control strategies in the presence of carriers. *J. Appl. Math*. 2023:1-14.

Luo Q and Han J 2022 Preparedness for a monkeypox outbreak. *Infect. Med*. 124–134.

Majee S, Jana S, Barman S and Kar T 2023 Transmission dynamics of monkeypox virus with treatment and vaccination controls: A fractional-order mathematical approach. *Phys. Script*. 98(2): 024002.

Martínez JI, Montalbán EG, Bueno SJ, Martínez FM, Juliá AN, Díaz JS, Marín NG, Deorador EC, Forte AN, García MA and Navarro AM 2022 Monkeypox outbreak predominantly affecting men who have sex with men. *Eurosurveillance*. 27(27):2200471.

Masoumnezhad M, Rajabi M, Chapnevis A, Dorofeev A, Shateyi S, Kargar NS and Nik HS 2020 An approach for the global stability of a mathematical model of an infectious disease. *Symmetry*. 12(11): 1778–1797.

Mbuthia FK and Chepkwony I 2019 Mathematical modeling of tungiasis disease dynamics incorporating hygiene as a control strategy. *J. Adv. Math. Comput. Sci.* 33(5): 1–8.

McCollum AM, Hill A, Shelus V, Traore T, Onoja B, Nakazawa Y and Lewis R 2023

Epidemiology of human monkeypox (Mpox)-worldwide, 2018-2021. 29-36.

Murphy H and Ly H 2022 The potential risks posed by inter-and intraspecies transmissions of monkeypox virus. *Virulence*. 13(1): 1681–1683.

Neilan RM and Lenhart S 2010 An introduction to optimal control with an application in disease modeling. *In Modeling Paradigms and Analysis of Disease Transmission Models* (pp. 67–81).

Olaniyi S, Lawal MA and Obabiyi OS 2016 Stability and sensitivity analysis of a deterministic epidemiological model with pseudo-recovery. *Int. J. Appl. Math*. 46 (2):160–167.

Olaniyi S and Chuma F 2023 Lyapunov stability and economic analysis of monkeypox dynamics with vertical transmission and vaccination. *International Journal of Applied and Comput. Math*. 9(5): 1–28.

Onyejekwe OO, Tigabie A, Ambachew B, Alemu A, et al. 2019 Application of optimal control to the epidemiology of dengue fever transmission. *J. Appl. Math. Phys*. 7(01): 148.

Perasso A 2018 An introduction to the basic reproduction number in mathematical epidemiology. *ESAIM: Proceedings Surveys*. 62: 123–138.

Peter OJ, Kumar S, Kumari N, Oguntolu FA, Oshinubi K and Musa R 2021 Transmission dynamics of monkeypox virus: a mathematical modelling approach. *Model. Earth Syst. Environ.* 2021:1–12.

Rahman MT, Sobur MA, Islam MS, Ievy S, Hossain MJ, El Zowalaty ME, Ashour HM 2020 Zoonotic diseases: aetiology, impact, and control. *Microorganisms* 8(9): 1405.

Railian M, Chumachenko T, Zubrii O and Nechyporuk I 2023 Assessing the current threat of monkeypox epidemic emergence. *WHO* 23 (2.1): 73–78. DOI:10.31718/2077-1096.23.2.1.73

Rangasamy M, Chesneau C, Martin-Barreiro C and Leiva V 2022 On a novel dynamic of SEIR epidemic models with a potential application to COVID-19. *Symmetry* 14(7): 1436.

Rimoin AW, Mulembakani PM, Johnston SC, Lloyd Smith JO, Kisalu NK, Kinkela TL and others 2010 Major increase in human monkeypox incidence 30 years after smallpox vaccination campaigns cease in the Democratic Republic of Congo. *Proc. Nat. Acad. Sci.* 107(37): 16262–16267.

Rizk JG, Lippi G, Henry BM, Forthal DN and Rizk Y 2022 Prevention and treatment of monkeypox. *Drugs*. 1–7.

Seang S, Burrel S, Todesco E, Leducq V, Monsel G, Le Pluart D, Palich R 2022 Evidence of human-to-dog transmission of monkeypox virus. *The lancet*. 400(10353): 658 –659.

Shaheen N, Diab RA, Meshref M, Shaheen A, Ramadan A, and Shoib S 2022 Is there a need to be worried about the new monkeypox virus outbreak? a brief review on the monkeypox outbreak. *Ann. Med. Surgery*. 104396.

Shao P and Shateyi S 2021 Stability analysis of SEIRS epidemic model with nonlinear incidence rate function. *Mathematics*. 9(21): 2644-2659.

Somma SA and Akinwande NI 2020 Sensitivity analysis for the mathematical modelling of monkeypox virus incorporating quarantine and public enlightenment campaign. *Fulafia J. Sci. Technol.* 6 (1):54–61.

Somma SA, Akinwande NI, and Chado UD 2019 A mathematical model of monkeypox virus transmission dynamics. *Ife J. Sci*. 21(1): 195–204.

Sudarmaji N, Kifl N, Hermansyah A, Yeoh SF, Goh BH and Ming LC 2022 Prevention and treatment of monkeypox: a systematic review of preclinical studies. *Viruses*. 14(11): 2496.

Syafruddin S and Noorani MSM 2013 Lyapunov function of sir and SEIR model for transmission of dengue fever disease. *Int. J. Simul. Proc. Model.* 8 (2-3): 177–184.

Titanji BK, Tegomoh B, Nematollahi S, Konomos M and Kulkarni PA 2022 Monkeypox: A contemporary review for healthcare professionals. *In Open Forum Infect. Diseases*. Vol.9(7):310.

Ugwa KA, Agwu I and Akuagwu N 2013

Mathematical analysis of the endemic equilibrium of the transmission dynamics of tuberculosis. *Int. J. Sci. Technol. Res*. 2(1): 263–269.

Upadhayay S, Arthur R, Soni D, Yadav P, Navik U, Singh R, ... Kumar P 2022 Monkeypox infection: the past, present, and future. *Int. Immunopharmacol*. 113: 109382.

Usman S and Adamu II 2017 Modeling the transmission dynamics of the monkeypox virus infection with treatment and vaccination interventions. *J. Appl. Math. Phys.* 5(12): 2335-2353.

Velavan TP and Meyer CG 2022 Monkeypox 2022 outbreak: An update.

Vera MN, Sanca K and Leon SR 2022 Comment on Sah et al. Monkeypox and its possible sexual transmission: Where are we now with its evidence? *Pathogens*. 11(8): 924-933.

WHO 2022 Disease outbreak news; multi-country monkeypox outbreak in non-endemic countries. Available at https://www.who.int/emergencies/disease-outbreak-news/item/2022-DON385.

WHO 2023 Mpox (monkeypox) - Democratic Republic of the Congo. Accessed at https://www.who.int/emergencies/disease-outbreak-news/item/2023-DON493.

Yan C, Jia J and Jin Z 2014 Dynamics of an SIR epidemic model with information variable and limited medical resources revisited. *Discrete Dynam. Nat. Soc*. 2014:1-11.

Yusuf TT and Benyah F 2012 Optimal control of vaccination and treatment for an SIR epidemiological model. *World J. Model. Simul.* 8(3): 194–204.